A global map of wood density

Fabian Jörg Fischer[1 2 3], Jérôme Chave[2], Amy Zanne[4], Tommaso Jucker[1], Alex Fajardo[5 6 7], Adeline Fayolle[8 9], Renato Augusto Ferreira de Lima[10], Ghislain Vieilledent[11 12 13], Hans Beeckman[14], Wannes Hubau[14 15], Tom De Mil[16 14], Daniel Wallenus[14], Ana María Aldana[17], Esteban Alvarez-Dávila[18], Luciana F. Alves[19], Deborah M. G. Apgaua[20], Fátima Arcanjo[21 22], Jean-François Bastin[23], Andrii Bilous[24], Philippe Birnbaum[25], Volodymyr Blyshchyk[24], Joli Borah[26], Vanessa Boukili[27 28], J. Julio Camarero[29], Luisa Casas[30], Roberto Cazzolla Gatti[31], Jeffrey Q. Chambers[32], Ezequiel Chimbioputo Fabiano[33], Brendan Choat[34], Edgar Cifuentes[35 17], Georgina Conti[36], David Coomes[37], Will Cornwell[38], Javid Ahmad Dar[39 40], Ashesh Kumar Das[41], Magnus Dobler[42], Dao Dougabka[43], David P. Edwards[44 45], Urs Eggli[46], Robert Evans[47], Daniel Falster[48], Philip Fearnside[49], Olivier Flores[50], Nikolaos Fyllas[51], Jean Gérard[52 53], Rosa C. Goodman[54], Daniel Guibal[52 53], L. Francisco Henao-Diaz[17 55], Vincent Hervé[56], Peter Hietz[57], Jürgen Homeier[58 59], Thomas Ibanez[60], Jugo Ilic[61 62], Steven Jansen[63], Rinku Moni Kalita[64 41], Tanaka Kenzo[65], Liana Kindermann[42], Subashree Kothandaraman[66 67], Martyna Kotowska[68 69], Yasuhiro Kubota[70 71], Patrick Langbour[52 53], James Lawson[72], André Luiz Alves de Lima[73], Roman Mathias Link[74], Anja Linstädter[42], Rosana López[75], Cate Macinnis-Ng[76], Luiz Fernando S. Magnago[77], Adam R. Martin[78], Ashley M. Matheny[79], James K. McCarthy[80], Regis B. Miller[81], Arun Jyoti Nath[82], Bruce Walker Nelson[83], Marco Njana[84], Euler Melo Nogueira[85 86], Alexandre Oliveira[87], Rafael Oliveira[88], Mark Olson[89], Yusuke Onoda[90], Keryn Paul[91], Daniel Piotto[92], Phil Radtke[93], Onja Razafindratsima[94], Tahiana Ramananantoandro[95], Jennifer Read[96], Sarah Richardson[80], Enrique G. de la Riva[97], Oris Rodríguez-Reyes[98 99], Samir G. Rolim[92], Victor Rolo[100], Julieta A. Rosell[101], Sassan Saatchi[102 103 104], Roberto Salguero-Gómez[105 106], Nadia S. Santini[107 108], Bernhard Schuldt[74 109], Luitgard Schwendenmann[110], Arne Sellin[111], Timothy Staples[112], Pablo R Stevenson[17], Somaiah Sundarapandian[113], Masha T van der Sande[114], Hans ter Steege[115 116], Shengli Tao[117 118], Bernard Thibaut[119], David Yue Phin Tng[20], José Marcelo Domingues Torezan[22], Boris Villanueva[120 121], Aaron Weiskittel[122], Jessie Wells[123], S. Joseph Wright[124], Kasia Zieminska[125] and Alexander Zizka[126]

Corresponding author: f.fischer@bristol.ac.uk

Affiliations

[1]School of Biological Sciences, University of Bristol, Bristol, BS8 1TQ United Kingdom

[2]Centre de Recherche Biodiversité Environnement, UMR 5300 (CNRS/IRD/UPS/INPT), 31062 Toulouse Cedex 9, France

[3]Technical University of Munich, School of Life Sciences, Ecosystem Dynamics and Forest Management in Mountain Landscapes, Hans-Carl-von-Carlowitz-Platz 2, 85354 Freising, Germany

[4]Cary Institute of Ecosystem Studies, Millbrook, NY 12545, USA

[5]Direccion de Investigación, Vicerrectoría Academica, Universidad de Talca, Campus Lircay, Talca, 3460000 Chile

[6]Instituto de Ecología y Biodiversidad (IEB), Las Palmeras 3425, Ñuñoa, 8310000 Chile

[7]Millenium Nucleus of Patagonian Limit-of-Life (LiLi), Valdivia 5090000, Chile

[8]Université de Liège, Gembloux Agro-Bio Tech, Gembloux, Belgium

[9]CIRAD, UPR Forêts et Sociétés, F-34398 Montpellier, France

[10]Departamento de Ciências Biológicas, ESALQ, Universidade de São Paulo, Avenida Pádua Dias, 11, 13418-900 Piracicaba, Brazil

[11]AMAP, Université de Montpellier, CIRAD, CNRS, INRAE, IRD, Montpellier, France

[12]CIRAD, UMR AMAP, F-98848 Nouméa, Nouvelle-Calédonie, France

[13]IAC, Nouméa, Nouvelle-Calédonie

[14]Service of Wood Biology, Royal Museum for Central Africa, Tervuren, Belgium

[15]Department of Forest and Water Management, Laboratory of Wood Technology, Ghent University, Ghent, Belgium

[16]Forest Is Life, TERRA Teaching and Research Centre, Gembloux Agro Bio-Tech, University of Liège, Gembloux

[17]Laboratorio de Ecología de Bosques Tropicales y Primatología, Universidad de Los Andes, 111711, Bogotá D.C, Colombia

[18]Fundacion Con Vida, Medellín, Colombia

[19]Center for Tropical Research, Institute of the Environment and Sustainability, UCLA, Los Angeles, CA, USA

[20]Centre for Rainforest Studies, The School for Field Studies, Yungaburra Qld 4872, Australia

[21]Universidade Federal de Uberlândia, Uberlândia, BR

[22]Biodiversity and Ecosystem Restoration Lab, Londrina State University, Campus Universitario, CCB, BAV, 86.051-990 Londrina, PR, Brazil

[23]TERRA Teaching and Research Centre, Gembloux Agro Bio-Tech, Université de Liège, Liège, Belgium

[24]National University of Life and Environmental Sciences of Ukraine (NUBiP), 03041 Kyiv, Ukraine

[25]CIRAD, UMR AMAP, F-34398 Montpellier, France. AMAP, Univ Montpellier, CIRAD, CNRS, INRAE, IRD, Montpellier, France

[26]Department of Animal and Plant Sciences, University of Sheffield, Sheffield, UK

[27]Department of Ecology and Evolutionary Biology, University of Connecticut, Storrs, CT, USA

[28]Office of Strategic Planning and Community Development, Somerville, Massachusetts, USA

[29]Instituto Pirenaico de Ecología (IPE-CSIC), Avda. Montañana 1005 50192, Zaragoza, Spain

[30]Laboratorio de Ecología de Bosques Tropicales y Primatología, Fundación Natura Colombia, Universidad de Los Andes, 111711, Bogotá D.C, Colombia.

[31]Department of Biological, Geological and Environmental Sciences, University of Bologna, Bologna, Italy

[32]University of California, Berkeley, Departement of Geography, Berkeley, CA, United States

[33]Department of Wildlife Management and Tourism Studies, University of Namibia Katima-Mulilo Campus, Ngweze, Katima-Mulilo 1096, Namibia

[34]Hawkesbury Institute for the Environment, Western Sydney University, Richmond, New South Wales, Australia

[35]Department of Plant Sciences, University of Cambridge, Cambridge, CB2 3EA, UK

[36]Instituto Multidisciplinario de Biología Vegetal (IMBIV), CONICET - Universidad Nacional de Córdoba, Edificio de Investigaciones Científicas y Técnicas, Av. Vélez Sársfield 1611, (CP5000), Córdoba, Argentina

[37]Conservation Research Institute and Department of Plant Sciences, University of Cambridge, Cambridge, CB2 3EA, UK

[38]School of Biological, Earth and Environmental Sciences, University of New South Wales, Sydney, Australia

[39]Terrestrial Ecology and Modelling (TEaM) Lab, Department of Environmental Science and Engineering, SRM University-AP, Amaravati-522240, Andhra Pradesh, India

[40]Centre for Geospatial Technology, SRM University-AP, Amaravati-522240, Andhra Pradesh, India

[41]Department of Ecology and Environmental Science, Assam University, Silchar 788 011, India

[42]Biodiversity Research and Systematic Botany, Institute of Biochemistry and Biology, Faculty of Science, University of Potsdam, 14469 Potsdam, Germany.

[43]École Nationale Supérieure des Travaux Publics du Tchad, Département des Sciences Fondamentales, BP 60, N'Djamena, Tchad

[44]Department of Plant Sciences and Centre for Global Wood Security, University of Cambridge, Cambridge, CB2 3EA, UK

[45]Conservation Research Institute, University of Cambridge, Cambridge, CB2 3EA, UK

[46]Sukkulenten-Sammlung Zürich / Grün Stadt Zürich, Mythenquai 88, 8002 Zürich, Switzerland

[47]School of Agriculture, Food and Ecosystem Sciences, University of Melbourne, Burnley Campus, Boulevard Drive, Richmond, Victoria 3121, Australia

[48]Evolution and Ecology Research Centre, University of New South Wales, Sydney New South Wales 2052, Australia.

[49]National Institute for Research in Amazonia (INPA), Manaus, Amazonas, Brazil

[50]Université de La Réunion, UMR PVBMT, Saint-Pierre, Reunion, France

[51]Department of Biology, Section of Ecology and Taxonomy, Athens, Greece

[52]CIRAD, UPR BioWooEB, F-34398 Montpellier, France

[53]BioWooEB, Univ Montpellier, Cirad Montpellier France

[54]Department of Forest Ecology and Management, Swedish University of Agricultural Sciences (SLU), Umeå, Sweden

[55]University and Jepson Herbaria, University of California Berkeley, USA

[56]Université Paris-Saclay, INRAE, AgroParisTech, UMR SayFood, 91120, Palaiseau, France

[57]Institute of Botany, Department of Ecosystem Management, Climate and Biodiversity, BOKU University, Vienna, Austria

[58]Faculty of Resource Management, HAWK University of Applied Sciences and Arts, Daimlerstraße 2, 37075 Göttingen, Germany

[59]Plant Ecology and Ecosystems Research, Georg-August University of Göttingen, 37073 Göttingen, Germany

[60]AMAP, Univ Montpellier, CIRAD, CNRS, INRAE, IRD, Montpellier, France

[61]University of New South Wales - School of Biological, Earth and Environmental Sciences - Evolution & Ecology Research Centre - Faculty of Science

[62]The University of Melbourne, Department of Forest and Ecosystem Science

[63]Institute of Botany, Ulm University, Albert-Einstein-Allee 11, 89081 Ulm, Germany

[64]Department of Botany, Bhattadev University, Bajali, Assam, India 781325

[65]Japan International Research Center for Agricultural Sciences, Tsukuba, Ibaraki, 305-8686, Japan

[66]Terrestrial Ecology and Modelling (TEaM) Lab, Department of Environmental Science and Engineering, SRM University-AP, Amaravati-522502, Andhra Pradesh, India

[67]Centre for Geospatial Technology, SRM University-AP, Amaravati-522502, Andhra Pradesh, India

[68]School of Natural Sciences, Macquarie University, Sydney, Australia

[69]Dept of Plant Ecology and Ecosystems Research, Albrecht-von-Haller Inst. for Plant Sciences, Univ. of Goettingen, Göttingen, Germany

[70]Think Nature Inc., Urasoe City, Japan.

[71]Faculty of Science, University of the Ryukyus, Nishihara, Japan.

[72]Climate and Natural Resources Group, NSW Department of Primary Industries and Regional Development, Ourimbah, NSW, Australia

[73]Federal Rural University of Pernambuco, Serra Talhada Academic Unit, CEP: 56909-535, Serra Talhada, PE, Brazil

[74]Forest Botany, Technical University of Dresden, Pienner Straße 7, 01737 Tharandt, Germany

[75]Departamento de Sistemas y Recursos Naturales, Escuela Técnica Superior de Ingenieros de Montes, Universidad Politécnica de Madrid, 28040, Madrid, Spain

[76]School of Biological Sciences and Te Pūnaha Matatini, Waipapa Taumata Rau, University of Auckland, Auckland, 1010 New Zealand

[77]Universidade Federal do Sul da Bahia, Centro de Formação em Ciências Agroflorestais, Praça José Bastos, s/n, Centro, 45600-923 Itabuna, BA, Brazil

[78]Department of Physical and Environmental Sciences, University of Toronto Scarborough, Toronto, Ontario, Canada

[79]Jackson School of Geosciences, Department of Earth and Planetary Sciences, University of Texas at Austin, United States of America

[80]Manaaki Whenua – Landcare Research, Lincoln, New Zealand

[81]Self-employed

[82]Department of Ecology and Environmental Science, Assam University, Silchar 788011, Assam, India

[83]Instituto Nacional de Pesquisas da Amazônia, Manaus, AM, BR

[84]Wildlife Conservation Society, Tanzania Country Program, Nature-Based Solutions, P. O Box 5196, Dar es Salaam, Tanzania

[85]Centro Universitário UniFG, Av. Governador Nilo Coelho, 4911, São Sebastião, Guanambi, Bahia, CEP 46430-000, Brazil

[86]Colégio Estadual Francisco Moreira Alves. Jaborandi-Bahia.

[87]Universidade de São Paulo, Instituto de Biociências, Cidade Universitária, São Paulo, SP, Brazil

[88]Universidade Estadual de Campinas, Departamento de Biologia Vegetal, Instituto de Biologia, Centro de Ecologia Integrativa, Campinas, Brazil

[89]Departamento de Botánica, Instituto de Biología, Universidad Nacional Autónoma de México, Ciudad de México, Mexico

[90]Division of Forest and Biomaterials Sciences, Graduate School of Agriculture, Kyoto University, Kyoto 606-8502, Japan

[91]CSIRO Environment, Canberra, Australian Capital Territory, Australia

[92]Centro de Formação em Ciências Agroflorestais, Universidade Federal do Sul da Bahia, BR 415, km 29, Ilhéus, BA 45613-204, Brazil

[93]Department of Forest Resources & Environmental Conservation, Virginia Tech, 319E Cheatham Hall, Blacksburg, VA 24061, USA

[94]University of California Berkeley, Berkeley, USA

[95]University of Antananarivo, Ecole Supérieure des Sciences Agronomiques, Mention Foresterie et Environnement, BP 175 Antananarivo 101, Madagascar

[96]School of Biological Sciences, Monash University, Victoria 3800, Australia

[97]Area de Ecología, Facultad de Ciencias Biológicas y Ambientales, Departamento de Biodiversidad y Gestión Ambiental, Universidad de León, Campus de Vegazana s/n, 24071, León, Spain

[98]Smithsonian Tropical Research Institute, Ancón, Panama City, Panama

[99]Instituto de Ciencias Ambientales y Biodiversidad, Universidad de Panamá, Estafeta Universitaria, Panamá

[100]Forest Research Group, INDEHESA, University of Extremadura, Plasencia, Spain

[101]Laboratorio Nacional de Ciencias de la Sostenibilidad, Instituto de Ecología, Universidad Nacional Autónoma de México, Tercer Circuito sn de Ciudad Universitaria, Mexico City, 04510, Mexico

[102]Jet Propulsion Laboratory, California Institute of Technology, Pasadena, CA, United States

[103]Ctrees, Pasadena, CA, United States

[104]Center for Tropical Research, Institute of the Environment and Sustainability, University of California Los Angeles, Los Angeles, CA, United States

[105]Department of Biology, University of Oxford, Oxford, United Kingdom

[106]Pembroke College, University of Oxford, Oxford, United Kingdom

[107]Instituto de Geología, Universidad Nacional Autónoma de México, Circuito de la Investigación Científica, Ciudad Universitaria, C.P. 04510, Ciudad de México, México

[108]Laboratorio Nacional de Geoquímica y Mineralogía, Universidad Nacional Autónoma de México, Circuito de la Investigación Científica, Ciudad Universitaria, C.P. 04510, Ciudad de México, México

[109]Plant Ecology, Albrecht von Haller Institute for Plant Sciences, University of Goettingen, Untere Karspüle 2, D-37073 Göttingen, Germany

[110]School of Environment, University of Auckland, Auckland, New Zealand

[111]Institute of Ecology and Earth Sciences, University of Tarty, Tartu, Estonia

[112]School of the Environment, The University of Queensland, St Lucia, Queensland, Australia

[113]Department of Ecology and Environmental Sciences, Pondicherry University, Puducherry, 605014, India

[114]Forest Ecology and Forest Management Group, Wageningen University & Research, Wageningen, The Netherlands

[115]Naturalis Biodiversity Center, Leiden, The Netherlands

[116]Quantitative Biodiversity Dynamics, Faculty of Science, Utrecht University, Utrecht, The Netherlands

[117]Institute of Ecology, College of Urban and Environmental Sciences, Peking University, Beijing 100871, China

[118]State Key Laboratory for Vegetation Structure, Function and Construction (VegLab), Peking University, Beijing 100871, China

[119]LMGC, Univ Montpellier, CNRS, Montpellier, France

[120]Universidad del Tolima GIBDET

[121]Jardín Botánico de Bogotá

[122]Center for Research on Sustainable Forests, University of Maine, Orono, ME 04469, USA

[123]School of Geography, Earth and Atmospheric Sciences, The University of Melbourne, Parkville, Victoria, Australia

[124]Smithsonian Tropical Research Institute, Balboa, Republic of Panama

[125]Independent researcher

[126]Department of Biology, Philipps University Marburg, Karl-von-Frisch-Straße 8, Marburg, 35043 Germany

1 **Abstract**

2 Wood density influences how quickly woody plants grow, how long they live and how

3 much carbon they store, yet its global variation remains poorly mapped. Here we

4 combined 109,626 wood density measurements from 16,829 species with 300,949

5 vegetation plots to produce a km-scale map of community-weighted wood density for

6 every woody biome. Our model led to a prediction accuracy 32–51 % higher than previous

7 global products, and a 1.8–3.7-fold wider wood density range (0.28–1.00 g cm^{-3}; global

8 mean: 0.57 g cm^{-3}) than previously assumed. Spatial cross-validation showed low bias

9 (±2.5 % of the mean), and uncertainties decreased from 20% in poorly sampled drylands

10 and boreal regions to 5% in data-rich temperate forests. Mean annual temperature was

11 the best predictor of community-weighted mean wood density, increasing by

12 0.01 g cm^{-3} for every 1°C change. We deliver a low-bias, high-resolution wood density

13 layer for Earth system models, together with spatially explicit error maps. This study

14 represents a major step forward for carbon accounting and trait-based forecasts of

15 vegetation change.

16

17 **Keywords:** wood density, aridity, carbon, functional traits, map, spatial autocorrelation,

18 temperature

19   The world's woody vegetation plays a major role in the global carbon cycle. It sequesters

20   and stores carbon and, in doing so, slows down anthropogenic climate change[1].

21   Monitoring and protecting carbon stocks is an essential mitigation strategy[2,3] and has

22   been enshrined in policy commitments[4]. However, we still lack a reliable global

23   quantification system for carbon storage in live vegetation[5]. Such a system requires wall-

24   to-wall quantification of the volume of woody plants and the density of their wood (dry

25   mass per unit green volume; g cm^{-3}). Volume estimates are rapidly improving thanks to a

26   growing array of air- and spaceborne sensors[6–8], but measuring wood density relies on

27   species identification and tissue extraction on the ground[9]. This process is labor-intensive

28   and leaves massive data gaps: species composition and mean wood densities are mostly

29   unobserved by satellites, potentially biasing carbon estimates[10]. It is thus critical to bridge

30   gaps in wood density information with robust statistical models.

31   Several wood density maps have been produced at global[11–13] and regional[14–16]

32   scales, but three types of inconsistencies are hampering efforts towards comparability

33   across maps. First, wood density cannot be measured for every single plant in a focal area,

34   meaning values must be estimated[17]. Studies differ in how they generate estimates, what

35   databases they draw on and how they standardize wood density values[18]. Second, studies

36   use different definitions and datasets to aggregate wood density at the level of ecological

37   communities. To account for species that are more abundant or biomass-rich than others,

38   community means are usually obtained by weighting the contribution of all individuals in

39   a focal area equally or in proportion to their cross-sectional (or basal) trunk area[19]. These

40   community-weighted means appear robust to the choice of weights[15], but require

41   comprehensive field inventories, which are rare, so studies often use geographically

42   imbalanced inputs[11], include unevenly and partially sampled communities[12,13], or average

43   directly across species occurrence records[16]. Third, modelling wood density across spatial

44 scales represents a great challenge. At broad scales, community-weighted mean wood

45 density varies with floristic composition[19], reflecting shifts in ecological strategies

46 between taxonomic groups (e.g., angiosperms vs. gymnosperms), life forms (e.g.,

47 succulents vs. non-succulents) and among species within these groups. All else being

48 equal, plants with high wood density are expected to be shorter and grow slower in

49 volume than less dense plants[20–22]. During early ecological succession, these high wood

50 density plants are at a disadvantage in the competition for light, but in the long run, high

51 wood density reduces hydraulic and mechanical risks and increases competitive ability[23].

52 We thus expect low mean wood densities in fast-turnover environments, such as under

53 frequent cycles of disturbance or recovery, or on fertile soils[24–27], and high wood densities

54 in hot and dry areas[28–30]. However, it is a major challenge to select appropriate predictors

55 and account for spatial autocorrelation in model calibration and validation[31].

56   Here, we map community-weighted mean wood density at 1 km^2 resolution

57 globally, mindful of the three challenges outlined above. To produce the map, we used a

58 major update of the Global Wood Density Database (GWDD v.2)[32], which contains over 6x

59 times as many wood density records (109,626) as the original and over 2x as many

60 species (16,829), all rigorously quality-checked and standardized[33]. We then compiled a

61 geographically balanced dataset of 300,949 vegetation inventories with detailed floristic

62 information across all woody biomes and used it to compute community-weighted wood

63 density, here defined as mean wood density weighted by basal area. Third, we mapped

64 community-weighted mean wood density with random forest models across the globe at

65 1 km^2 resolution. We selected 10 environmental predictors with biologically meaningful

66 links to wood density variation, thoroughly validated the wood density map, and

67 compared it with three published global maps[11–13] as well as a regional map[15]. Our results

68   represent a major step forward in creating a reliable global carbon quantification system

69   and improving climate change assessments.

70

71 **Results**
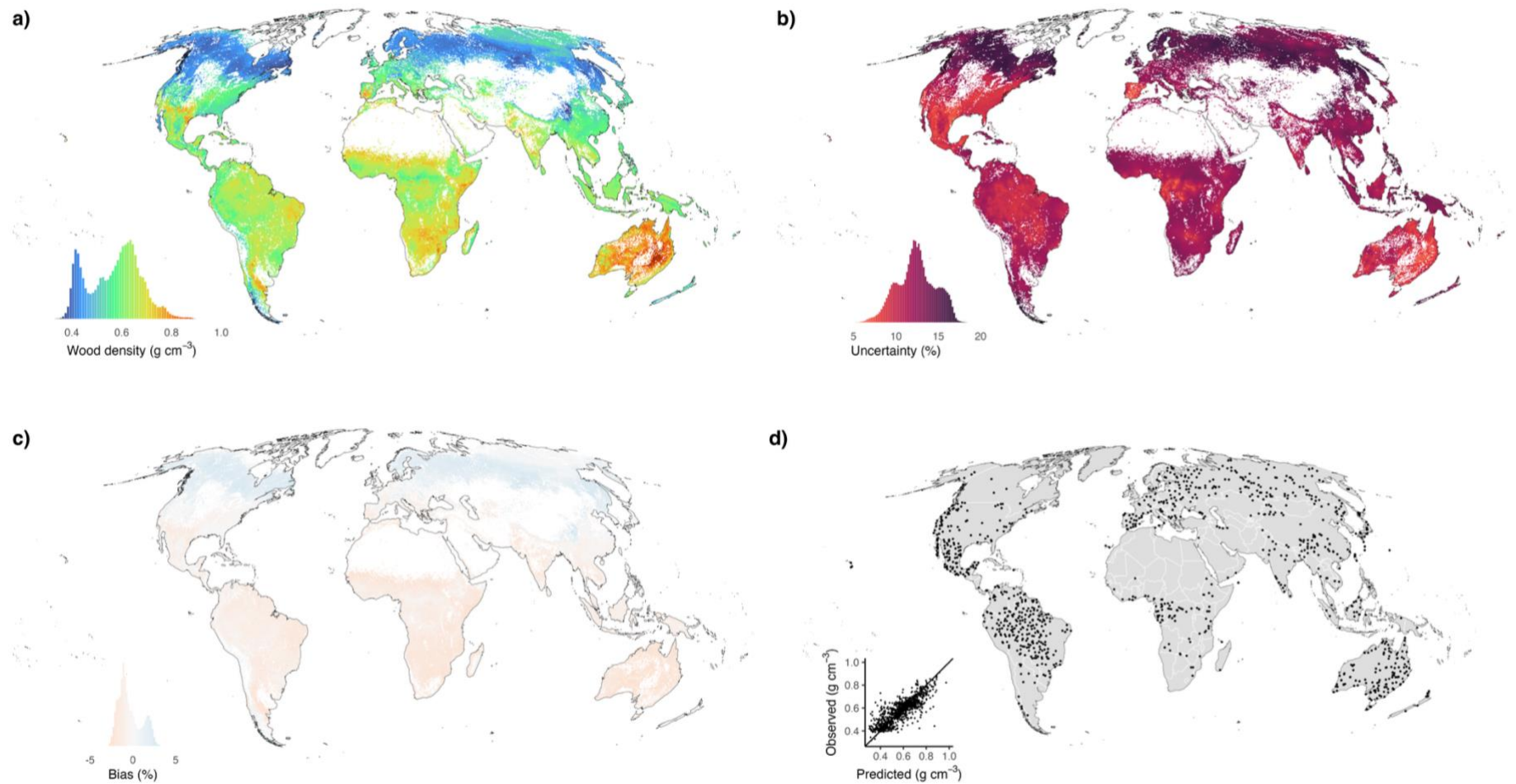
72 *Global distribution of community-weighted mean wood density*

73 Community-weighted mean wood density varied more than 3-fold from 0.28 g cm^{-3} to

74 1.00 g cm^{-3} across the globe, with a mean of 0.57 g cm^{-3} and standard deviation of 0.104 g

75 cm^{-3} (95% confidence interval, 95%CI: 0.40 to 0.77 g cm^{-3}, n_{pixel} = 86.7 million, Fig. 1a).

76 Values displayed a bimodal distribution with one mode at 0.42 g cm^{-3}, reflecting

77 gymnosperm-dominated forests at high latitudes, and a second mode at 0.64 g cm^{-3},

78 reflecting tropical forests and savannas (Fig. 1a, Table S1). Dry biomes, such as deserts

79 and xeric shrublands had the highest average densities at 0.66 g cm^{-3} (95%CI: 0.47 to 0.79

80 g cm^{-3}, Table S1), but also large biogeographic variation. Our map predicted much higher

81 average wood densities of 0.76 g cm^{-3} (95%CI: 0.64 to 0.87 g cm^{-3}) than the dry-biome

82 average across xeric environments in Australia and much lower densities of 0.46 g cm^{-3}

83 (95%CI: 0.40 to 0.63 g cm^{-3}) in succulent-dominated Baja California. In the boreal zone,

84 larch-dominated forests of Northeast Siberia exceeded the boreal average by ca. 20%,

85 with wood densities of 0.50 g cm^{-3} (95%CI: 0.43 to 0.63 g cm^{-3}).

86

87 *Map validation and error assessment*

88 To create spatially explicit estimates of uncertainty and bias, we performed a spatially

89 stratified cross-validation. We selected a geographically balanced subset of 1,000 plots

90 (median area: 0.64 ha, Fig. 1d), compared modelled and observed wood densities, and

91 used the results to map uncertainty (Fig. 1b) and mean error (or bias, Fig. 1c). Overall bias

92 was low, at -0.003 g cm^{-3} (95%CI: -0.017 to 0.009), or -0.4% (-2.3 to 2.3, Table S2) of the

93 predicted wood density. The mean uncertainty was 0.069 g cm^{-3} (or 12.4%, Fig. S2), and

94 it varied substantially across space (95%CI: 0.049 to 0.087 g cm^{-3}, or 8.0 to 16.5%).

95 To assess the importance of spatial autocorrelation, we tested how uncertainty

96 depended on the distance of predictions from training samples (Table S3). Prediction

97 errors were lowest directly adjacent to training data (0.043 g cm^{-3}, i.e., 7.8% for a

98 reference wood density of 0.55 g cm^{-3}, Tables S4-5) but increased when training data were

99 100 km away (0.065 g cm^{-3}, or 11.8%). Spatial autocorrelation reduced at larger distances,

100 but uncertainty still increased up to 0.080 g cm^{-3} (14.5%) at 1,000 km. Random Forest

101 models, our default approach, captured this spatial structure more effectively than linear

102 regression models, but differences between approaches were small when modelled

103 residuals were spatially interpolated (Fig. S3-4).

104 Uncertainties in community-weighted wood density were lowest in regions such

105 as USA, which are densely sampled, with a mean uncertainty of 0.053 g cm^{-3} (10.4%, n_{pixel}

106 = 7.0 million) and a 95% range from 0.048 to 0.067 g cm^{-3} (7.0 to 15.5%, locally down to

107 5%). By contrast, in South Africa, uncertainty reached 0.086 g cm^{-3} (12.8% of the mean,

108 n_{pixel} = 0.8 million) and varied from 0.079 to 0.092 g cm^{-3} (11.2 to 13.7%). The highest

109 relative uncertainties (up to 15-20%) were observed in the boreal zone where mean

110 wood density was low and plot coverage was sparser than in the temperate zone (Table

111 S2, Fig. 1b, Fig. S12). There was some evidence for regional prediction biases, such as

112 underestimation at high and overestimation at low wood densities, but both were low, in

113 the range of 0.01-0.02 g cm^{-3} (Fig. 1c and Fig. S5, Table S2).

114

Fig. 1: Global maps of wood density, prediction errors and validation plots. Shown is the predicted global distribution of community-weighted mean wood density (g cm^{-3}, a), relative prediction uncertainty (% of predicted wood density, b), relative prediction bias (% of predicted wood density, c) and the validation plots (d). Maps have a 1 km resolution in Mollweide equal area projection. In panels a-c, insets show both the colour scale and the histogram of values. In panel d, the inset shows predicted vs. observed wood densities for all validation plots in basic cross-validation (i.e., not accounting for distance to training data). Areas without tree or shrub cover are masked. For absolute uncertainty and bias maps see Fig. S5. In panels b and c, colour scale breaks have been matched to cover the same 5% intervals.

120 *Environmental and biogeographic determinants of wood density*

121 The most important predictor of community-weighted mean wood density variation was

122 mean annual temperature (Fig. 2a, Fig. S6, Table 1). For an increase in temperature by one

123 standard deviation (sd_{MAT} = 7.24°C), wood density increased by 0.075 g cm^{-3} (multiple

124 regression model, 95% CI from 0.075 to 0.076), or roughly by 0.01 g cm^{-3} for a 1°C change.

125 Site water balance was the next most important predictor (Fig. 2b, Table 1), with

126 increasing water availability leading to a decrease in wood density (-0.012 g cm^{-3}, 95% CI

127 from -0.012 to -0.012, no change due to rounding, Fig. S6). These patterns were robust to

128 substitution to other climatology layers (Table S1). Wood density further showed

129 consistent, but moderate decreases of -0.017 g cm^{-3} with cyclone frequency (-0.017 to -

130 0.017) and gymnosperm proportion (-0.018 to -0.017), but their importance was low for

131 wood density mapping (Table 1).

132
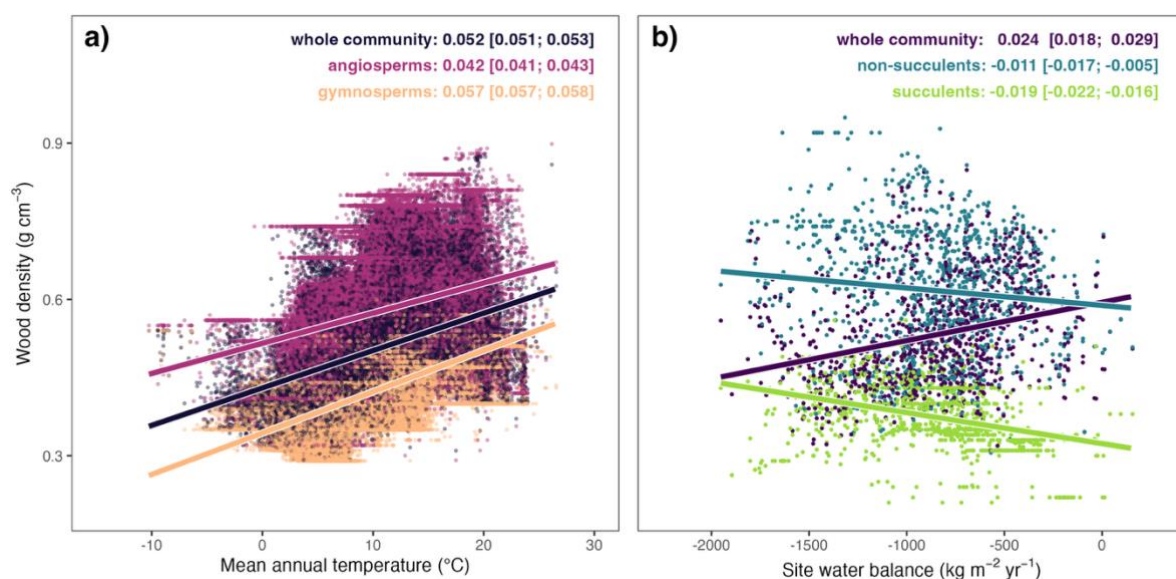
Fig. 2: Examples of environmental wood density variation across phylogenetic groups and life forms.
Panel a: relationship between mean annual temperature (°C) and community-weighted mean wood density
(g cm^{-3}) for plots where angiosperms and gymnosperms co-exist (n = 249,354). Wood density varies with
temperature for angiosperms and gymnosperms separately as well as when both groups are combined
("whole community"). Lines are linear regression lines for each subset. The corresponding slope estimates
and 95% CIs are provided in the top right corner. For comparability across predictors, slope estimates are
reported with respect to standardized mean annual temperature, i.e., in units of g cm^{-3} for one standard

140   deviation shift in temperature (sd_{MAT} = 7.24°C). Panel b: relationship between site water balance, an

141   indicator of water availability for plant growth (sd_{SWB} = 320 kg m^{-2} yr^{-1}, details in Table S6) and community-

142   weighted mean wood density across communities with co-occurring succulents and non-succulents (n =

143   3,108). Succulents were defined broadly as trees or tree-like plants with any type of succulent habit (e.g.,

144   Baobab, Aloe tree, Saguaro). This includes stem-water storage and succulent roots or leaves. Note that wood

145   density decreases with water availability in both subgroups in panel b, but increases when the subgroups

146   are aggregated, which is due to decreasing succulent presence at high water availability (Simpson's

147   paradox). Such effects reduce predictive power when modelling community-weighted means (cf. Fig. S6b).

148

149   To assess the consistency and utility of temperature and aridity for wood density

150   mapping, we computed temperature and aridity effects in two subgroups (Fig. 2),

151   representing differences in xylem structure and leaf habit (angiosperms vs.

152   gymnosperms) and drought resistance strategies (succulent vs. non-succulent woody

153   plants). In mixed forests, wood density increased with temperature both at aggregate

154   level (0.052 g cm^{-3}, 95%CI: 0.051 to 0.053, simple linear regression) and separately in

155   gymnosperms and angiosperms (0.057 g cm^{-3} and 0.042 g cm^{-3}, with 95%CIs from 0.057

156   to 0.058, and from 0.041 to 0.043, respectively). Wood density also decreased with

157   increasing water availability in co-occurring succulent (-0.019 g cm^{-3} for site water

158   balance, -0.022 to -0.016) and non-succulent plants (-0.011 g cm^{-3}, -0.017 to -0.005), but

159   the declining presence of succulents in areas with higher water availability reversed the

160   effect at aggregate levels (Fig. 2b).

Layer	Pearson's r	Simple regression coefficient	Multiple regression coefficient	Importance (spatial RF validation)
Mean annual temperature (°C)	0.57	0.060 [0.060, 0.061]	0.075 [0.075, 0.076]	18
Site water balance (kg m^{-2} year^{-1})	-0.22	-0.024 [-0.024, -0.023]	-0.012 [-0.012, -0.012]	5
Soil sand content (g kg^{-1})	-0.03	-0.003 [-0.003, -0.003]	-0.003 [-0.003, -0.002]	4
Burned area (%)	0.03	0.003 [0.003, 0.004]	-0.004 [-0.005, -0.004]	3
Deciduous angiosperms proportion (%)	-0.04	-0.004 [-0.005, -0.004]	0.015 [0.014, 0.015]	3
Elevation (m)	-0.17	-0.019 [-0.019, -0.018]	0.013 [0.013, 0.014]	2
Gymnosperm proportion (%)	-0.45	-0.048 [-0.048, -0.047]	-0.017 [-0.018, -0.017]	1

Mean wind speed (m s^{-1})	-0.20	-0.022 [-0.022, -0.021]	0.011 [0.011, 0.012]	1
Cation exchange capacity (mmol(c) kg^{-1})	-0.33	-0.035 [-0.035 -0.034]	0.006 [0.006, 0.007]	0
Cyclone frequency (yr^{-1})	-0.04	-0.005 [-0.005, -0.004]	-0.017 [-0.017, -0.017]	0

161 **Table 1. Predictor importance and effect sizes for wood density mapping.** Shown are 10 predictors

162 used to create the global map of community-weighted mean wood density, their bivariate correlation with

163 wood density (Pearson's r), their effect size in a multiple regression model (g cm^{-3}) and their importance in

164 a random forest model (cf. methods). All predictors were standardized, so effect sizes correspond to shifts

165 in wood density (in g cm^{-3}) for a change of one standard deviation of the predictor variable. Predictors are

166 sorted from most important to least important. This approach downweighs predictors with regional effects

167 (e.g., cyclone frequency). Sources and definitions of the predictors can be found in Table S6. Correlations

168 between predictors (Pearson's r < 0.6 throughout) are shown in Figure S13.

169

170 *Comparison with alternative mapping approaches*

171 We found that the present map was a significant improvement compared to previous

172 mapping approaches. Uncertainty was reduced by 13% (ratio of variances) compared to

173 a map produced with the previous GWDD (Fig. S7, uncertainty of 0.074 g cm^{-3}, 95%

174 interval from 0.49 to 0.99), and previous regional biases, such as an overestimation of

175 wood densities across Australia (0.077 g cm^{-3} or 10.3% of mean wood density), were

176 reduced to less than 2.5% (Fig. 1c). The present map also considerably improved over

177 three published global wood density maps (Table S7), two of which calculated mean wood

178 density directly from samples without weighting by basal area ("Boonman2020"[12] and

179 "Yang2024"[13]) and one that used the same definition of community-weighted means as

180 our study ("Mo2024"[11]). There were similarities with the published maps in terms of

181 global means (0.55 to 0.56 g cm^{-3}) and qualitative trends (R^2 of 0.60 to 0.83, Fig. S8-10,

182 Table S7). However, our study revealed a 1.8-3.7 times larger spatial variation in wood

183 density than published previously (Table S7), and we also improved mapping accuracy,

184 reducing uncertainty by 51% compared to Boonman2020, 45% compared to Yang2024,

185 and 32% compared to Mo2024.

186   Improvements were also noticeable regionally. Over Amazonian forests, we found

187   a clear increase from 0.59 g cm^{-3} (95%CI: 0.55 to 0.63) in Southwest Amazon moist forests

188   to 0.65 g cm^{-3} (95%CI: 0.61 to 0.69) in Guiana lowland moist forests (Fig 3a). This result

189   replicated trends in the raw plot data (0.58 vs. 0.66 g cm^{-3}) and a regional map (albeit

190   weaker, Fig. S11). Overall, predictive power was low (R^2 = 0.26), but comparable to the

191   regional map (Fig. S11) and considerably higher than in previously published maps (R^2 =

192   0.03-0.05), which predicted little to no variation across the Amazon (Fig. 3, b-d).

193
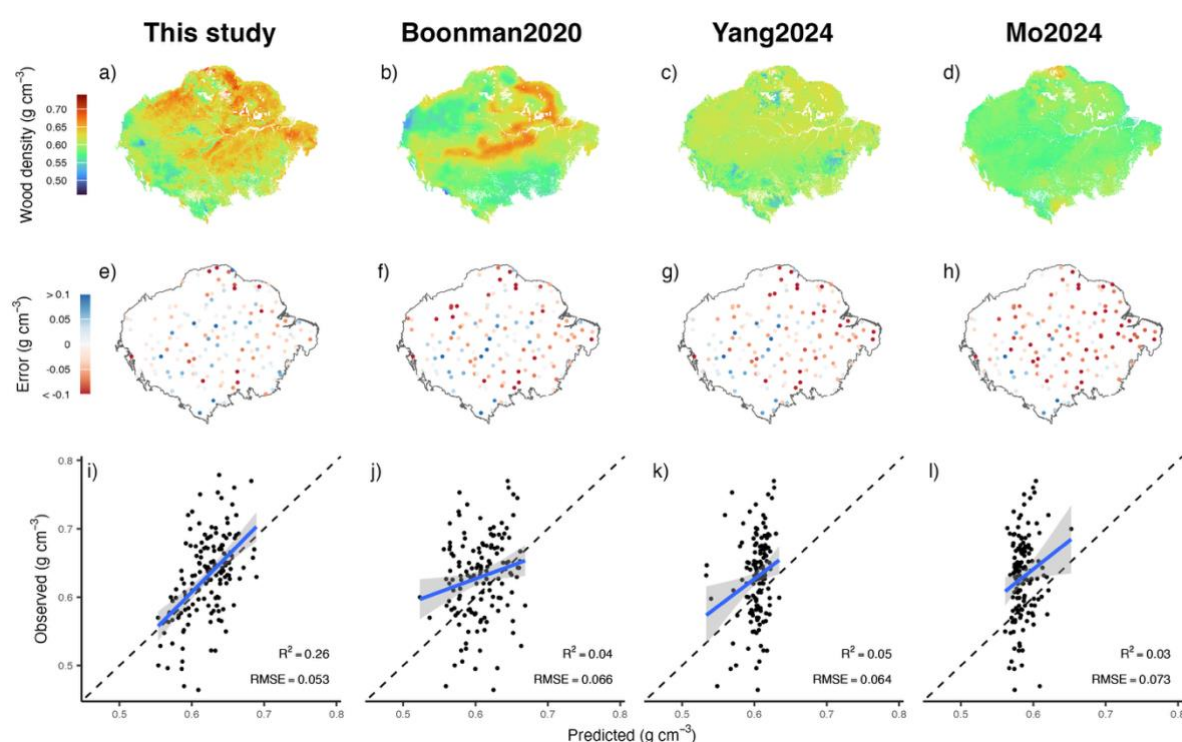
194   **Fig. 3: Wood density variation across Amazonian forests, as predicted from global wood density**

195   **maps.** Shown is the wood density gradient across Amazonia, as predicted by the present study and three

196   published global maps (panels a-d), their errors across validation plots (e-h), and a plot of observed vs.

197   predicted wood densities (i-l, n = 152, Fig. 1d). All depicted quantities are in g cm^{-3}. Errors are computed

198   via cross-validation (e and i) or direct map-plot comparisons (f-h and j-l). Blue lines in panels i-l are least

199   squares regression lines with 95%CI envelopes. Note that variation in the validation data occurs at much

200   smaller scales (~1 ha plots) than the prediction scale (~1 km^2 pixels), which may explain why R^2 values are

201   low and observed wood density ranges larger in the validation data (approx. 0.45 to 0.8 g cm^{-3}) than in any

202   of the maps. For a comparison with a local wood density map, the same plot can be found in Fig. S11.

203   **Discussion**

204   Here we mapped community-weighted mean wood density at global scale using a

205   combination of wood density measurements and vegetation inventories, including nearly

206   17,000 species and more than 300,000 plot locations. The new wood density map

207   achieved 32-51% higher accuracy than previous studies, revealed a 1.8-3.7 times larger

208   variation and displayed clear environmental and biogeographic patterns. Our findings

209   underscore the tight coupling between wood density and fundamental plant-ecological

210   strategies[29], which makes it a valuable predictive trait for modelling vegetation

211   composition and dynamics across landscapes and through time[34]. We also carried out a

212   detailed, spatial assessment of prediction errors, which revealed low biases (±2.5 % of the

213   mean), and uncertainties ranging from 20% in the most poorly sampled regions to 5% in

214   the best-sampled regions. Our work provides a critical improvement since wood density

215   is a key component of carbon accounting at landscape[35,36], regional[10] and global scales[7,11],

216   requiring comprehensive, spatially explicit error budgets.

217   Our results differed from previous global studies that did not account for plant size

218   when averaging at community-level[12,13], but also outperformed an existing map of

219   community-weighted mean wood density[11] (Fig. 3, Figs. S8-10). Most of these

220   discrepancies likely stemmed from the improved spatial coverage of plot collection in the

221   present study and from the much larger and curated collection of wood density estimates

222   of the GWDD v.2. By contrast, the inclusion of heavily human-modified forests in earlier

223   training sets[11] is unlikely to explain the narrower variance in those maps: strong

224   anthropogenic disturbance would be expected to increase wood density variation among

225   communities, not reduce it[37]. The performance and spatial patterns of the new map were

226   more comparable to those seen in regional maps[15], but there were still notable

227   mismatches, for example in the strength and extent of gradients across Amazonia (Figure

228   S11). To address these differences, future mapping efforts may benefit from considering

229   additional soil and disturbance variables, which are expected to be the main drivers of

230   wood density variation across Amazonia[14,15].

231   The study at hand also showed that community-weighted mean wood density

232   followed predictable patterns across large environmental gradients. Given balanced and

233   high-quality inputs, most patterns could be predicted from a few biologically informative

234   variables, potentially reducing the need for large predictor sets and complex model

235   tuning[11,13,38]. For example, for an increase in temperature by one standard deviation,

236   wood density was estimated to increase by 0.075 g cm^{-3}, or by 0.01 g cm^{-3} for a 1°C change.

237   Conversely, wood density decreased by -0.012 g cm^{-3} with a change in one standard

238   deviation of site water balance, the second most important predictor. This confirmed the

239   hypothesis that higher exposure to heat and drought stress favours slow-growing plants

240   with dense wood[28]. There were regional deviations, e.g., high wood densities both in the

241   driest (Sahel) and wettest parts (Congo Basin) of tropical Africa, but the strong and

242   consistent relationship of community-level wood density with temperature was

243   surprising (Fig. 2a). Temperature effects on wood density have rarely been explained

244   physiologically[39], and while they also exist at the species and intraspecific level, they

245   usually remain less pronounced than the effects of water availability[33,38]. A possible

246   explanation is that aridity tends to limit which strategies are viable in terms of building

247   woody tissues, while temperature tends to determine which strategies are successful, e.g.,

248   at high aridity, plants with high wood density increasingly become viable, but, due to low

249   growth rates, they do not dominate biomass accumulation until heat stress is also high.

250   Global warming and increasing drought stress may thus lead to a reshaping of plant

251   communities towards higher wood densities. To date, however, empirical studies do not

252   support such a densification trend or even suggest the opposite pattern[40].

253　　　　More generally, the interpretation of environmental effects on wood density is

254　　complex. Climate variables such as temperature are linked to multiple stressors, and

255　　wood density is a compound trait that also summarizes several wood anatomical

256　　properties, including those of vessels, fibres and parenchyma cells[41], and correlates with

257　　whole-plant architecture[42,43]. Links between wood density and the environment may thus

258　　arise indirectly[44], or be mediated by tradeoffs[45], trait-trait covariation[46], and tree size[47].

259　　Soluble organic compounds, so-called "extractives", can also be a confounding factor, as

260　　they are usually not removed during wood density determination[48]. They have negligible

261　　impact on carbon estimates, as they account for a small share of stem biomass in most

262　　plants and possess carbon contents comparable to wood (40-50%)[49]. However, they may

263　　bias relationships between wood density and environmental factors and explain regional

264　　anomalies, such as the comparatively high wood densities in forests of extractive-rich

265　　larches[50] across Siberia (Fig. 1a).

266　　　　A key concern in mapping biological quantities across space is spatial

267　　autocorrelation, which comes about, for example, due to dispersal limitations of

268　　organisms, or unmodelled spatial variation in climatic and edaphic predictors, and which

269　　influences both model fitting[51] and testing[31]. Here, prediction uncertainty in random

270　　forest models increased with distance from training data over the entire range that we

271　　tested, i.e., from 1 to 1,000 km, and most clearly (by 129%) up to 100 km. This finding

272　　reveals that a considerable portion of predictive power is due to spatial autocorrelation,

273　　far more than suggested by previous studies[11]. Confirmation of this result was provided

274　　by multiple regression models, which were generally inaccurate ($R^2 \sim 0.3$, Fig. S4), but

275　　improved substantially when spatially interpolated residuals were added to predictions

276　　(R^2 up to 0.75). While spatial autocorrelation is often seen as a confounding factor in

277　　ecology, it also presents an opportunity to correct predictions through careful sampling

278   protocols and spatial interpolation. For example, we estimated accuracy to be highest

279   across systematically sampled regions such as USA (0.048 g cm^{-3}, or down to 5%).

280   Therefore, investment in gridded field data collections in poorly sampled regions (e.g.,

281   through national forest inventories and/or extension of plot networks) holds one of the

282   keys to producing high-quality wood density and carbon maps[9].

283   This study suggests two possible areas of improvement. Stressful environments

284   spur a wide variety of strategies in plants to reduce mortality risks[52]. Wood density maps

285   may considerably improve in accuracy if trade-offs between these strategies and wood

286   density are better accounted for and more accurate predictor maps are created. In our

287   study, succulents showed the same increase in wood density with aridity as co-occurring

288   non-succulents (Fig. 2b). However, the generally light-wooded succulents increasingly

289   dominated in dry areas – likely due to water storage and the often-co-occurring,

290   transpiration-efficient CAM photosynthesis[53] –, which reversed the relationship with

291   aridity at aggregate levels (Simpson's paradox, Fig. S6b). Similar patterns could emerge

292   for other stress-resistance or stress-avoidance strategies (e.g., deciduousness), meaning

293   reliable maps of stressors, life forms and growth habits are needed for wood density

294   mapping.

295   Second, a large proportion of wood density variation occurs at scales smaller than

296   1 km[10], reflecting the fine-scale mosaics of disturbance[37] and species composition[19]. This

297   scaling difference led to high uncertainties (low R^2) when predicting wood density at plot-

298   level from maps at km scales (Fig. 3). However, high-resolution forest age maps are now

299   available[54,55], and leveraging these maps together with high-resolution canopy heights

300   maps[56], would help map fine-scale wood density variation[36]. The present study will

301   provide a robust foundation for future efforts and will help improve the accuracy of land

302   carbon monitoring and vegetation modelling.

Methods

Wood density data assembly

We assembled an updated version of the Global Wood Density Database[32], GWDD v.2[33], which reports basic wood density, defined as oven-dried mass of a wood sample divided by its green volume[48] in g cm^{-3}. We employed the same wood density definition as in the original GWDD and, to maximize taxonomic coverage, included both measurements of individual plants and averages across several individuals. We used a broad definition of wood that includes tissues from tree-like plants that lack secondary growth, such as palms and succulents. We included direct measurements of basic wood density but also wood density values obtained at different moisture levels, which were transformed to basic wood density via physical conversion factors[18]. Taxonomic records were standardized via the *WorldFlora* package[57] in R[58], based on World Flora Online (www.worldfloraonline.org, June 2023 release), an international initiative that supersedes *The Plant List*[59]. Fuzzy matches of taxon names were manually checked and corrected where necessary. The final database contains 109,626 records from 16,829 species, with coverage across biomes and biogeographic realms[33].

Plot data assembly

To weight wood density by relative species dominance, we assembled a global collection of 300,949 vegetation inventories – plots with taxonomic identification and measurements of stem diameter for all sampled plants – from 300,702 unique 1 km x 1 km cells and 281 sources (Table S8, Fig. S12). We privileged old-growth and intact forests and, where identifiable, excluded data from woody ecosystems with strong anthropogenic impacts. We selected primarily ecological studies from protected areas, excluded heavily managed stands from national forest inventories and plantations of non-native species,

328   such as eucalypts planted outside of Australia. Woody ecosystems such as xeric

329   environments with succulents or shrubs were included, with no minimum threshold in

330   woody cover, to represent the full range of wood density variation.

331   For each plot, we defined the community-weighted wood density CWWD by

332   averaging across individuals i as follows:

333
$$CWWD = \frac{\sum_i wd_i BA_i}{\sum_i BA_i} = \frac{\sum_i wd_i D_i^2}{\sum_i D_i^2}$$

334   Here wd_i is the wood density of individual i, $BA_i = \frac{\pi}{4} D_i^2$ its cross-sectional (or basal) area

335   and D_i its trunk diameter. This weighting scheme gives considerably more weight to

336   species with large canopy trees than a simple aggregation across all individuals (i.e.,

337   weighting by species abundance), but less than weighting by tree volume, since the latter

338   depends not only on basal area, but also tree height, which also increases with trunk

339   diameter[60]. While weighting schemes subtly shift the interpretation of the typical traits of

340   communities, in practice, community-weighted means of wood density have proven

341   robust to how different size classes are weighted[15,31], and basal-area weighting remains a

342   widely used and practical approach[19].

343   The majority of the CWWD values were computed from open access raw data on

344   tree- or species level basal area (n = 243,776). We also identified geographical data gaps–

345   primarily dry ecosystems in South America, South and East Africa, India –, and

346   supplemented the collection with published surveys from these areas. Additional

347   geographic gaps were filled by direct CWWD estimates from the literature, especially in

348   tropical forests[10,31,61] and in Russian forests[62]. Some of these published CWWD values

349   have been computed from the original GWDD, so they may carry over some biases due to

350   conversion factors[18], but they fill an important knowledge gap and were therefore

351   retained. Most of the surveys included trees measured at 10 cm in trunk diameter and

352 above, but this threshold varied from 1 up to 30 cm in some locations. This should not

353 systematically bias wood density estimates, since community-weighted means tend to be

354 robust to the choice of weighting factors[15] and since large trees disproportionally

355 contribute to basal area and woody volume[31].

356 Inventory data were matched to wood density values from the GWDD v.2 at the

357 species and genus level following standard procedures[63]. Only plots with wood density

358 values for >80% of the total basal area were retained. If two or more plots from the same

359 source fell into the same 1 km x 1 km grid cell (Mollweide equal-area projection,

360 ESRI:54009), their CWWD values were averaged to produce a cell-wide CWWD estimate

361 using the *terra* package[64]. To do this, plots were averaged by weighting by their total basal

362 area.

363

364 *Wood density mapping*

365 To map wood density, we assembled 10 climatic, disturbance and auxiliary layers (full

366 definitions in Table S6), and resampled them to the 1 km x 1 km Mollweide grid also used

367 for aggregating wood density estimates. We chose predictors in accordance with

368 biological hypotheses about the determinants of wood density variation (stress,

369 disturbance, soil fertility), including climatic variables for the period 1981-2010 from

370 CHELSA/BIOCLIM+[65,66], edaphic factors[67], disturbance agents such as fire[68] and broad-

371 scale community composition[69]. We also derived cyclone frequency from the best track

372 archive[70] by counting how often each 1 km x 1 km grid cell was within a 150 km radius of

373 a cyclone track and normalizing this number by the number of years. Pairwise

374 correlations between predictors never reached r = 0.6, which minimizes collinearity

375 issues with attributing effects when modelling and mapping wood density[71].

376   Based on the set of 10 predictors, we applied random forest models to predict

377   wood density at 1 km x 1 km resolution. We used the *ranger* package[72]. To account for

378   spatial autocorrelation in wood density variation and improve predictions, we added

379   spatially interpolated residuals to the final map, relying on the 25 nearest plots for each

380   grid cell and using inverse distance weighting (1/r, where r is a plot's distance from the

381   target grid cell) via the R packages *terra* and *gstat*[73]. For comparison, we also retained the

382   map without spatially interpolated residuals. We repeated the procedure with a multiple

383   regression model with the same 10 predictors, again creating maps both with and without

384   spatially interpolated residuals. We mapped wood density across all land pixels globe but

385   then masked pixels without any woody plants (0% tree or shrub cover), using a mask

386   from the Copernicus Global Land Cover product[74].

387

388   *Map validation*

389   We validated the map using a subset of 1,000 plots, selected as follows. We chose a

390   minimum sampling area of 0.25 ha to reduce noise, then selected plots via geographic

391   stratification to avoid biasing validation towards regions of denser sampling. To this end,

392   we subdivided the globe into 200 x 200 km grid cells, and randomly sampled one plot

393   from each grid cell. After having drawn once from each grid cell, continued drawing from

394   random grid cells until reaching 1,000 samples (Fig. S1). We selected 1,000 plots, as this

395   reflects well the distance between plots in sparsely sampled areas (~100-200 km) and

396   provides a large enough sample size to reduce randomness in validation.

397   Once the validation plots were selected, we carried out a spatial leave-one-out

398   (LOO) cross validation[31]. First, we carried out a standard LOO validation: for each of the

399   1,000 plots, we replicated the wood density map, including spatial interpolation of

400   residuals, based on all data except the validation plot itself and compared predicted

401 against observed wood density values. We then repeated this process three times, but

402 each time removed not only the validation plot from the training data, but also all data

403 points within an exclusion radius ranging between 1 and 1,000 km from the validation

404 plot.[30] We did not choose the exclusion radii as fixed thresholds (as in ref. [31]), but drew

405 them at random from a uniform distribution. This choice allowed us to assess spatial

406 autocorrelation continuously up to 1,000 km. A few duplicates occurred when randomly

407 drawn exclusion radii did not exclude any additional plots. We removed these predictions,

408 resulting in a total of 3,841 data points for validation.

409   To generate error estimates for each grid cell in the wood density map, we

410 modelled the error distribution depending on the predicted wood density, the distance

411 from the nearest five plots and the interaction of both (Table S3). The best fit to the data

412 was obtained by modelling uncertainty with a t location-scale or "student" distribution,

413 which is useful for modeling data distributions with heavier tails than the normal

414 distribution:

415
$$P(x) = C_{\sigma_t,\nu} \left(\frac{\nu}{\nu + (x/\sigma_t)^2} \right)^{(\nu+1)/2}$$
416

417 This distribution approaches the normal distribution as ν approaches infinity, while

418 smaller values of ν yield heavier tails. With this distribution, the variance is given by

419 $var = \sigma_t \times \nu/(\nu - 2)$. The fitting was performed with the package $brms$[75] and suggested

420 a shape parameter of either $\nu = 5$ or $\nu = 6$. To ensure comparable error structure across

421 models, we fixed $\nu = 5$ and then mapped both the mean error (bias) and uncertainty in

422 wood density. Uncertainty can be directly expressed via the σ_t parameter, but here we

423 report $\sigma_t^* = 1.11 \times \sigma_t$, which is comparable to the standard deviation of a normal

424 distribution, since 68.26% of data points lie within $[-\sigma_t^*, \sigma_t^*]$.

425

426   *Assessment of environmental determinants*

427   To evaluate the relative importance of environmental variables for wood density mapping

428   we re-created the global wood density map 10 times, each time dropping one of the

429   predictors, carrying out a spatial cross-validation and mapping uncertainty across woody

430   ecosystems. Predictors that, upon dropping, led to the largest loss of accuracy globally,

431   were considered the most important for the mapping. To reduce the computational

432   burden in spatial cross-validation, we created a reduced data set of n = 74,725 plots by

433   applying a 10 km x 10 km filter and selecting a single plot per grid cell for model training.

434   We verified that this choice had negligible impacts on model accuracy. For an assessment

435   of the direction of effects, we also computed simple linear regression models, with

436   community-weighted mean wood density regressed against each predictor separately,

437   and fitted a multiple linear regression model with the same predictors. More precisely,

438   we used the model $wd_i = \beta_0 + \sum_{j=1}^{10} \beta_j x_{ij} + \epsilon_i$, where wd_i is the community weighted

439   wood density of plot i, x_{ij} is predictor variable j for observation i, and ϵ_i is the residual for

440   observation i, distributed as $\epsilon_i \sim N(0, \sigma^2)$. Predictors were scaled to one standard

441   deviation to ensure comparability of effect sizes.

442   Climatic predictors were found to be the most important ones in predicting spatial

443   variation in wood density, so we decided to carry out two additional robustness tests.

444   First, we used the TerraClimate[76] and ERA5-Land[77] datasets in place of the CHELSA data

445   and evaluated changes in the global wood density map. In the case of mean annual

446   temperature and mean wind speed, we used like-for-like substitutions. In the case of

447   CHELSA's site water balance variable, there was no direct equivalent, so we chose other

448   aridity-related predictors, such as climatic water deficit, the difference between potential

449   and actual evapotranspiration (TerraClimate), and potential evapotranspiration (ERA5-

450   Land).

451   Variation in wood density was also found to depend on wood anatomy and plant

452   life forms. If either of those factors changed the effect of environmental predictors, not or

453   insufficiently accounting for them could induce bias and increase uncertainty in wood

454   density maps. We tested the consistency of predictions across gymnosperms and

455   angiosperms, as these are species-rich and globally dominant plant groups that differ in

456   wood anatomy and leaf habit, and across succulents and non-succulents, as water storage

457   in plant organs is a key drought-resistance strategy, which has often co-evolved with

458   transpiration-reducing CAM photosynthesis[53] and should lead to strong trade-offs with

459   wood density in dry regions[52]. For the former, we selected all plots with both angiosperms

460   and gymnosperms (n = 249,354, "mixed forests") and compared simple linear regression

461   estimates of community-weighted wood density against temperature within each plant

462   group and across groups. For the latter, we matched diameter measurements to a list of

463   succulents compiled from the literature[78–81] and compared regression estimates of

464   community-weighted wood density against site water balance both within each life form

465   and across life forms. The full list of succulent species with wood density records in the

466   GWDD v.2 can be found in Table S8. We did not distinguish between different types of

467   succulence, and defined succulents broadly as woody or wood-like plants with any type

468   of succulent habit.

469

470   *Comparison with wood density maps*

471   Finally, we compared the global wood density map to other products. First, we compared

472   it to a map created only from wood density records in the previous version of the GWDD[32].

473   We compared both maps in terms of overall uncertainty and assessed regional biases due

474   to lower species coverage and outdated conversion factors[18]. Second, we compared it to

475   three published maps[11–13]. Although two of these maps did not weight wood density by

476   tree size (basal area or volume), their estimates were explicitly aimed at representing

477   communities in terms of species dominance and carbon stocks[12,13], and should thus be

478   comparable with the community-weighted means used in this study. We resampled all

479   three maps to the same 1 km x 1 km Mollweide grid, then evaluated them in terms of

480   overall wood density distribution and against the same 1,000 spatially stratified

481   validation plots. We assessed correlations with the reference map via R^2, and predictive

482   performance on validation plots via root mean square errors (RMSE) and R^2. The latter

483   were compared to the RMSE and R^2 of the reference map under basic leave-one-out cross

484   validation (ratio of variances). Third, we assessed the ability of our reference map and the

485   three published maps to predict a known wood density gradient across Amazonian

486   rainforests[10]. We compared RMSEs and R^2 across plots from the global validation dataset

487   (Fig. 1d), but located within Amazonia (n = 152), and also compared predictions from this

488   study against a recently produced regional map [15] (Fig. S11).

489

490   **Acknowledgments**

500

555

556   **Competing Interests**

557   None declared.

558

559   **Author contributions**

560   F.J. Fischer, J. Chave and A. Zanne conceived of the project. F.J. Fischer led the assembly

561   and processing of the data, the analysis for the manuscript, and the writing of a first draft

562   of the manuscript, with assistance from J. Chave, A. Zanne, T. Jucker, A. Fajardo, A. Fayolle,

563   R.A.F. de Lima and G. Vieilledent. All co-authors contributed substantially through data

564   collection, data assembly and revisions of the manuscript.

565

566   **Data availability**

567   All data sources for this analysis are openly available. The GWDD v.2 will be made publicly

568   available on Zenodo (doi: 10.5281/zenodo.16919510) as part of a companion

569   manuscript. All code to reproduce the analyses and maps in this manuscript will be made

570   publicly available on Zenodo upon publication of this manuscript (doi:

571   10.5281/zenodo.16932871). The references for all data sources and the analysis scripts

572   are available in the Supplementary Information.

Literature

1. Friedlingstein, P. *et al.* Global Carbon Budget 2023. *Earth Syst Sci Data* **15**, 5301–5369 (2023).

2. Poorter, L. *et al.* Biomass resilience of Neotropical secondary forests. *Nature* **530**, 211–214 (2016).

3. Griscom, B. W. *et al.* Natural climate solutions. *Proceedings of the National Academy of Sciences* **114**, 11645–11650 (2017).

4. UNFCCC. Global Stocktake. (2025).

5. Ochiai, O. *et al.* Towards a roadmap for space-based observations of the land sector for the UNFCCC global stocktake. *iScience* **26**, (2023).

6. Quegan, S. *et al.* The European Space Agency BIOMASS mission: Measuring forest above-ground biomass from space. *Remote Sens Environ* **227**, 44–60 (2019).

7. Santoro, M. *et al.* The global forest above-ground biomass pool for 2010 estimated from high-resolution satellite observations. *Earth Syst Sci Data* **13**, 3927–3950 (2021).

8. Dubayah, R. *et al.* The Global Ecosystem Dynamics Investigation: High-resolution laser ranging of the Earth's forests and topography. *Science of Remote Sensing* 100002 (2020) doi:10.1016/j.srs.2020.100002.

9. Chave, J. *et al.* Ground Data are Essential for Biomass Remote Sensing Missions. *Surv Geophys* **40**, 863–880 (2019).

10. Mitchard, E. T. A. *et al.* Markedly divergent estimates of Amazon forest carbon density from ground plots and satellites. *Global Ecology and Biogeography* **23**, 935–946 (2014).

11. Mo, L. *et al.* The global distribution and drivers of wood density and their impact on forest carbon stocks. *Nat Ecol Evol* (2024) doi:10.1038/s41559-024-02564-9.

12. Boonman, C. C. F. *et al.* Assessing the reliability of predicted plant trait distributions at the global scale. *Global Ecology and Biogeography* (2020) doi:10.1111/geb.13086.

13. Yang, H. *et al.* Global patterns of tree wood density. *Glob Chang Biol* **30**, e17224 (2024).

14. ter Steege, H. *et al.* Functional composition of the Amazonian tree flora and forests. *Commun Biol* **8**, 355 (2025).

15. Sullivan, M. J. P. *et al.* Variation in wood density across South American tropical forests. *Nat Commun* **16**, 2351 (2025).

16. Šímová, I. *et al.* Spatial patterns and climate relationships of major plant traits in the New World differ between woody and herbaceous species. *J Biogeogr* **45**, 895–916 (2018).

17. Flores, O. & Coomes, D. A. Estimating the wood density of species for carbon stock assessments. *Methods Ecol Evol* **2**, 214–220 (2011).

18. Vieilledent, G. *et al.* New formula and conversion factor to compute basic wood density of tree species using a global wood technology database. *Am J Bot* **105**, 1653–1661 (2018).

19. Phillips, O. L. *et al.* Species Matter: Wood Density Influences Tropical Forest Biomass at Multiple Scales. *Surv Geophys* **40**, 913–935 (2019).

20. Olson, M. *et al.* Xylem vessel-diameter–shoot-length scaling: ecological significance of porosity types and other traits. *Ecol Monogr* **90**, e01410 (2020).

21. Fajardo, A. Wood density relates negatively to maximum plant height across major angiosperm and gymnosperm orders. *Am J Bot* **109**, 250–258 (2022).

22. Fajardo, A., Siefert, A. & Laughlin, D. C. Wood density and leaf size jointly predict woody plant growth rates across (but not within) species along a steep precipitation gradient. *Journal of Ecology* **112**, 374–388 (2024).

23. Kunstler, G. *et al.* Plant functional traits have globally consistent effects on competition. *Nature* **529**, 204–207 (2016).

24. Muller-Landau, H. C. Interspecific and inter-site variation in wood specific gravity of tropical trees. *Biotropica* **36**, 20–32 (2004).

25. King, D. A., Davies, S. J., Tan, S. & Noor, N. S. M. The role of wood density and stem support costs in the growth and mortality of tropical trees. *Journal of Ecology* **94**, 670–680 (2006).

26. Curran, T. J., Gersbach, L. N., Edwards, W. & Krockenberger, A. K. Wood density predicts plant damage and vegetative recovery rates caused by cyclone disturbance in tropical rainforest tree species of North Queensland, Australia. *Austral Ecol* **33**, 442–450 (2008).

27. Oliveira, G. M. V. *et al.* Behavior of wood basic density according to environmental variables. *J For Res (Harbin)* **33**, 497–505 (2022).

28. Hacke, U. G., Sperry, J. S., Pockman, W. T., Davis, S. D. & McCulloh, K. A. Trends in wood density and structure are linked to prevention of xylem implosion by negative pressure. *Oecologia* **126**, 457–461 (2001).

29. Chave, J. *et al.* Towards a worldwide wood economics spectrum. *Ecol Lett* **12**, 351–366 (2009).

30. Kraft, N. J. B., Metz, M. R., Condit, R. S. & Chave, J. The relationship between wood density and mortality in a global tropical forest data set. *New Phytologist* **188**, 1124–1136 (2010).

31. Ploton, P. *et al.* Spatial validation reveals poor predictive performance of large-scale ecological mapping models. *Nat Commun* **11**, (2020).

32. Zanne, A. E. *et al.* Data from: Global wood density database. *Dryad Digital Repository* (2009) doi:10.5061/dryad.234.

33. Fischer, F. J. *et al.* Beyond species means - the contribution of intraspecific variation to global wood density variation. *Manuscript submitted for publication* (2025).

34. van Bodegom, P. M., Douma, J. C. & Verheijen, L. M. A fully traits-based approach to modeling global vegetation distribution. *Proceedings of the National Academy of Sciences* **111**, 13733–13738 (2014).

35. Mascaro, J., Detto, M., Asner, G. P. & Muller-Landau, H. C. Evaluating uncertainty in mapping forest carbon with airborne LiDAR. *Remote Sens Environ* **115**, 3770–3774 (2011).

36. Jucker, T. *et al.* Topography shapes the structure, composition and function of tropical forest landscapes. *Ecol Lett* **21**, 989–1000 (2018).

37. Poorter, L. *et al.* Wet and dry tropical forests show opposite successional pathways in wood density but converge over time. *Nat Ecol Evol* **3**, 928–934 (2019).

38. Towers, I. R. *et al.* Revisiting the role of mean annual precipitation in shaping functional trait distributions at a continental scale. *New Phytologist* **241**, 1900–1909 (2024).

39. Thomas, D. S., Montagu, K. D. & Conroy, J. P. Changes in wood density of Eucalyptus camaldulensis due to temperature - The physiological link between water viscosity and wood anatomy. *For Ecol Manage* **193**, 157–165 (2004).

669   40.   Pretzsch, H., Biber, P., Schütze, G., Kemmerer, J. & Uhl, E. Wood density reduced
670   while wood volume growth accelerated in Central European forests since 1870.
671   *For Ecol Manage* **429**, 589–616 (2018).
672   41.   Ziemińska, K., Westoby, M. & Wright, I. J. Broad anatomical variation within a
673   narrow wood density range - A study of twig wood across 69 Australian
674   angiosperms. *PLoS One* **10**, (2015).
675   42.   Goodman, R. C., Phillips, O. L. & Baker, T. R. The importance of crown dimensions
676   to improve tropical tree biomass estimates. *Ecological Applications* **24**, 680–698
677   (2014).
678   43.   Jucker, T. *et al.* The global spectrum of tree crown architecture. *Nat Commun* **16**,
679   4876 (2025).
680   44.   Lachenbruch, B. & Mcculloh, K. A. Traits, properties, and performance: How
681   woody plants combine hydraulic and mechanical functions in a cell, tissue, or
682   whole plant. *New Phytologist* **204**, 747–764 (2014).
683   45.   Gleason, S. M. *et al.* Weak tradeoff between xylem safety and xylem-specific
684   hydraulic efficiency across the world's woody plant species. *New Phytologist* **209**,
685   123–136 (2016).
686   46.   Anderegg, L. D. L. *et al.* Within-species patterns challenge our understanding of the
687   leaf economics spectrum. *Ecology Letters* vol. 21 734–744 Preprint at
688   https://doi.org/10.1111/ele.12945 (2018).
689   47.   Olson, M. *et al.* Plant height and hydraulic vulnerability to drought and cold. *Proc
690   Natl Acad Sci U S A* **115**, 7551–7556 (2018).
691   48.   Williamson, G. B. & Wiemann, M. C. Measuring wood specific gravity...correctly.
692   *Am J Bot* **97**, 519–524 (2010).
693   49.   Matthews, G. *The Carbon Content of Trees. Forestry Commission Technical Paper 4.*
694   (1993).
695   50.   Côté, W. A., Day, A. C., Simson, B. W. & Timell, T. E. Studies on Larch
696   Arabinogalactan. I. The Distribution of Arabinogalactan in Larch Wood. **20**, 178–
697   192 (1966).
698   51.   F. Dormann, C. *et al.* Methods to account for spatial autocorrelation in the analysis
699   of species distributional data: a review. *Ecography* **30**, 609–628 (2007).
700   52.   Gross, N. *et al.* Unforeseen plant phenotypic diversity in a dry and grazed world.
701   *Nature* **632**, 808–814 (2024).
702   53.   Males, J. Secrets of succulence. *J Exp Bot* **68**, 2121–2134 (2017).
703   54.   Besnard, S. *et al.* Mapping global forest age from forest inventories, biomass and
704   climate data. *Earth Syst Sci Data* **13**, 4881–4896 (2021).
705   55.   Bourgoin, C. *et al.* Human degradation of tropical moist forests is greater than
706   previously estimated. *Nature* **631**, 570–576 (2024).
707   56.   Wagner, F. H. *et al.* High Resolution Tree Height Mapping of the Amazon Forest
708   using Planet NICFI Images and LiDAR-Informed U-Net Model. Preprint at
709   https://arxiv.org/abs/2501.10600 (2025).
710   57.   Kindt, R. WorldFlora: An R package for exact and fuzzy matching of plant names
711   against the World Flora Online taxonomic backbone data. *Appl Plant Sci* **8**, e11388
712   (2020).
713   58.   R Development Core Team. R: A Language and Environment for Statistical
714   Computing. *R Foundation for Statistical Computing* Preprint at
715   https://doi.org/10.1007/978-3-540-74686-7 (2021).
716   59.   The Plant List. The Plant List. Version 1.1. *Internet* (2013).

717 60. Niklas, K. J. The Scaling of Plant Height: A Comparison Among Major Plant Clades
718   and Anatomical Grades. *Ann Bot* **72**, 165–172 (1993).

719 61. Lewis, S. L. *et al.* Above-ground biomass and structure of 260 African tropical
720   forests. *Philosophical Transactions of the Royal Society B: Biological Sciences* **368**,
721   20120295 (2013).

722 62. Schepaschenko, D. *et al.* A dataset of forest biomass structure for Eurasia. *Sci Data*
723   **4**, (2017).

724 63. Réjou-Méchain, M., Tanguy, A., Piponiot, C., Chave, J. & Hérault, B. Biomass: an R
725   Package for Estimating Above-Ground Biomass and Its Uncertainty in Tropical
726   Forests. *Methods Ecol Evol* **8**, 1163–1167 (2017).

727 64. Hijmans, R. J. terra: Spatial Data Analysis. Preprint at https://CRAN.R-
728   project.org/package=terra (2023).

729 65. Karger, D. N. *et al.* Climatologies at high resolution for the earth's land surface
730   areas. *Sci Data* **4**, 170122 (2017).

731 66. Brun, P., Zimmermann, N. E., Hari, C., Pellissier, L. & Karger, D. N. Global climate-
732   related predictors at kilometer resolution for the past and future. *Earth Syst Sci
733   Data* **14**, 5573–5603 (2022).

734 67. Hengl, T. *et al.* SoilGrids250m: Global gridded soil information based on machine
735   learning. *PLoS One* **12**, (2017).

736 68. Chuvieco, E., Pettinari, M. L., Lizundia Loiola, J., Storm, T. & Padilla Parellada, M.
737   ESA Fire Climate Change Initiative (Fire_cci): MODIS Fire_cci Burned Area Grid
738   product, version 5.1. *Centre for Environmental Data Analysis* (2019)
739   doi:doi:10.5285/3628cb2fdba443588155e15dee8e5352.

740 69. Tuanmu, M.-N. & Jetz, W. A global 1-km consensus land-cover product for
741   biodiversity and ecosystem modelling. *Global Ecology and Biogeography* **23**,
742   1031–1045 (2014).

743 70. Knapp, K. R., Kruk, M. C., Levinson, D. H., Diamond, H. J. & Neumann, C. J. The
744   international best track archive for climate stewardship (IBTrACS). *Bull Am
745   Meteorol Soc* **91**, 363–376 (2010).

746 71. Dormann, C. F. *et al.* Collinearity: A review of methods to deal with it and a
747   simulation study evaluating their performance. *Ecography* **36**, 27–46 (2013).

748 72. Wright, M. N. & Ziegler, A. Ranger: A fast implementation of random forests for
749   high dimensional data in C++ and R. *J Stat Softw* **77**, 1–17 (2017).

750 73. Gräler, B., Pebesma, E. & Heuvelink, G. Spatio-temporal interpolation using gstat. *R
751   Journal* **8**, 204–218 (2016).

752 74. Buchhorn, M. *et al.* Copernicus Global Land Cover Layers—Collection 2. *Remote
753   Sens (Basel)* **12**, (2020).

754 75. Bürkner, P. C. Advanced Bayesian multilevel modeling with the R package brms. *R
755   Journal* **10**, 395–411 (2018).

756 76. Abatzoglou, J. T., Dobrowski, S. Z., Parks, S. A. & Hegewisch, K. C. TerraClimate, a
757   high-resolution global dataset of monthly climate and climatic water balance from
758   1958-2015. *Sci Data* **5**, 170191 (2018).

759 77. Muñoz-Sabater, J. *et al.* ERA5-Land: a state-of-the-art global reanalysis dataset for
760   land applications. *Earth Syst Sci Data* **13**, 4349–4383 (2021).

761 78. Eggli, U. *Illustrated Handbook of Succulent Plants: Dicotyledons*. (Springer Berlin
762   Heidelberg, 2004).

763 79. Eggli, U. & Nyffeler, R. *Illustrated Handbook of Succulent Plants. Dicotyledons:
764   Rosids*. (Springer International Publishing, Cham, 2023). doi:10.1007/978-3-030-
765   85239-9.

766   80.   Anderson, E. & Eggli, U. *Das Große Kakteen-Lexikon*. (Ulmer, 2005).

767   81.   Eggli, U. & Nyffeler, R. *Illustrated Handbook of Succulent Plants. Monocotyledons*.
768   (Springer Berlin Heidelberg, Berlin, Heidelberg, 2020). doi:10.1007/978-3-662-
769   56486-8.
770